Parallel Transceiver Array Design Using the Modified Folded Dipole for 7T Body Applications

Wonje Lee[1], Martijn Cloos[1], Daniel Sodickson[1], and Graham Wiggins[1]
[1]*Radiology, NYUMC, New York, NY, United States*

Introduction: Despite the SNR benefits of high fields, body imaging at 7T is challenging as major difficulties remain with strong B1 inhomogeneity, less penetration depth, complex Tx/Rx field patterns, and increased SAR [1]. TEM/microstrip coils are common in array design at UHF, capturing local electric fields between two conductors, but suffer from concomitant weak sensitivities deep in tissue due to the presence the shielding effect of the ground plane. In regions of signal voids caused by either field twisting or destructive field interactions, accurate B1 maps are difficult to obtain, limiting the effectiveness of B1 shimming and parallel transmit pulse design. Conventional loop designs also exhibit significant field twisting behavior in conductive objects at high fields [2]. To allow for effective excitations using a body array with a broad variety of pulse design methods, we adopt a new antenna design, the "modified-folded dipole" (mf-dipole) [3], as a transceiver array, and evaluate its performance in terms of efficiency compared to a bench mark coil [4]. Individual B1+/- field patterns of the array and initial in-vivo images with a 3 spoke pTx pulse for uniform excitation are also presented.

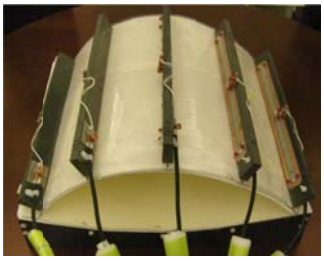

Fig.1 Photograph of 8ch mf-dipole array

Methods: The mf-dipole array consists of 8 elements, arranged in three posterior elements under the PVC frame with 40cm length and 45cm width, and five anterior elements on a flexible acrylic plate to accommodate various body shapes (fig.1). Elements were 32cm long, positioned 11cm apart, and all reasonably matched (S11 below -20 dB) and isolated (S21 below -18 dB) in the presence of the conductive object (Body size agar gel phantom, permittivity=77, conductivity=0.6 [S/m]). For imaging experiments the array was connected to an in-house TR switch box through two cable traps per element to suppress common mode currents. The array was interfaced to a 7T 8ch pTx system (Siemens, Magnetom) with capability of 1kW maximum peak power per channel. The bench mark coil, 8ch loop array with 2ch Tx/Rx & 8ch Rx was used for the efficiency comparison [4]. As a Tx performance metric the flip angle (FA) images on the axial center slice were obtained at the maximum available Tx reference voltage for both coils using the pre-saturation based B1 map [5].Phases to the 8 elements were specified such that they produce circular polarization at the center of the phantom , whereas the 2ch loops were optimally positioned to get the constructive B1 at the center with power from the single channel system split and phased by 180 degrees [4]. SNR maps for root sum of squares reconstruction were generated by acquiring 2D GRE images both with and without RF excitation. These maps were normalized for excitation flip angle distribution by dividing by the sine of the flip angle at each pixel. The individual B1+ maps (fig.4a) were calculated based on each FA distribution, normalized by its maximum, whereas the B1- maps were obtained by normalizing each 2D GRE image by the sine of the excitation flip angle at each pixel (fig.4b). After safety evaluations, in-vivo 2D GRE body images using the 3 spoke pTx pulses (based on DREAM B1 map sequence [7]) were attempted with breath holding, and compared to conventional circularly polarized excitation. (256x 256, TR/TE:20/4ms, BW:1028Hz/pix, Slice thick:5mm, FOV280mm) For the spoke pulse calculations two separate B1maps were obtained with the circular polarization(CP) and gradient mode (GM) shim sets that compensate null regions each other due to the orthogonal mode relations, enabling more reliable B1maps for each channel.

Results: At the maximum Tx power available the mf-dipole array provides 98 degree FA (fig.2a) in the centric region, compared to the 65 degree (fig.2b) using the optimized 2 loop transmit configuration. Assuming comparable total excitation power between two cases the mf-dipole array exhibits approximately 50 % improvement in Tx performance. On the receive side, the 8ch loop shows 7% better normalized SNR performance at the center (150 in fig.3b), compared to the mf-dipole array (140 in fig.3a), also exhibiting higher signals in the periphery (fig.3). Individual (fig.4a) B1+ and (fig.4b) B1- maps of the array are presented in figure 4, showing benign field twisting and monotonic field decay from the antenna. The uniform excitation using the 3 spoke pTx pulses, compared to the CP local shim set eliminates dark bands around both kidneys effectively (fig.5). The 3plane localizer images with the CP shim set demonstrate the broad FOV (450x450) of the array, suitable for body applications.

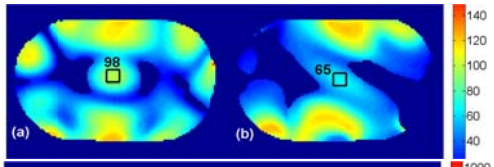

Fig.2 FA image at the max. Tx power available, (a) 8ch mf-dipole (b) 8ch loop (2ch Tx/Rx & 6ch Rx)

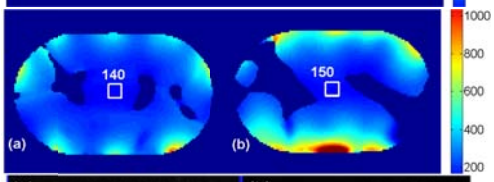

Fig.3 nSNR, (a) 8ch mf-dipole (b) 8ch loop (2ch Tx/Rx & 6ch Rx)

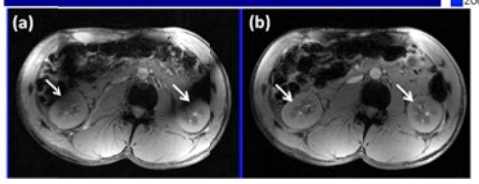

Fig.5 2D GRE axial images with (a) CP shim set (b) 3 spoke pTx pulse

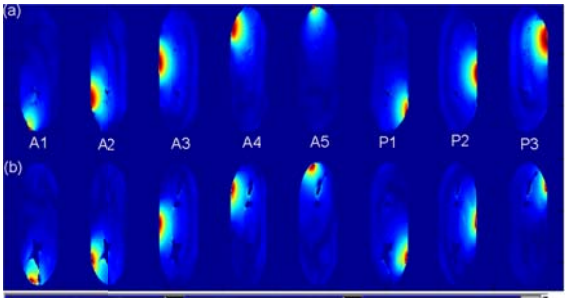

Fig.4 individual (a) B1+ (b) B1- patterns of the mf-dipole array

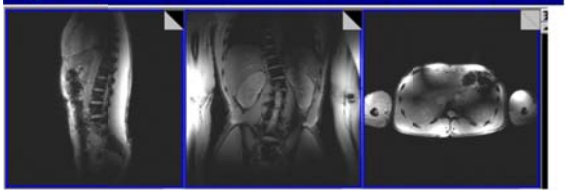

Fig.6 3plane localizer FOV 450 with the CP shim set

Discussions: Higher FA achieved using the mf-dipole array may be attributed not only to the benefits of the local phase shim but also to the in-phase current distribution of the mf-dipole structure, compared to a shielded stripline element where the current on the shield opposes the current on the element, contributing to enhanced sensitivity with depth. In addition, the uni-directional currents on its bifurcated legs may contribute to the benign field twisting as contrast to the TEM or the loop. The slight SNR degradation of the mf-dipole is possibly caused by the additional loss of the lumped inductors that might be replaced by distributed antenna layout design. Initial assessment of the uniform excitation using the tailored pTx pulse improves B1 homogeneity effectively thanks to the better B1 map acquisition method.

Reference [1] MRM 2012 **67**(4): 954-964 [2] ISMRM 20(2012) p2996 [3] ISMRM 21(2013) submitted [4] ISMRM 20(2012) p2782 [5] ISMRM 16(2008) p1247 [6] MRM 2005 54(6):1439–1447 [7] MRM 68(2012):1517-1526